Original article

HISTORICAL BRICKS DETERIORATION AND RESTORATION FROM THE RED MONASTERY, SOHAG, EGYPT: A GEOCHEMICAL, PETROLOGICAL AND STATISTICAL APPROACHES

Abd-Elkareem, E.[1], Ali, M.[2] & El-Sheikh, A.[2]

[1]*Conservation dept., Faculty of Archaeology, South Valley Univ., Qena, Egypt.*
[2]*Geology dept., Faculty of Sciences, Sohag Univ., Sohag, Egypt.*

E-mail: *elashmawyabdelkareem@yahoo.com*

Abstract

The present study investigates for the first time the historical bricks of The Red Monastery (west Sohag, Egypt), built about fifth century AD, which showing several aspects of brick decay. Several techniques were employed (geochemical, petrographical, mineralogical and morphological) to determine their deterioration features and provenance of the raw material as well as shed lights on the firing techniques. In addition, integration of geochemical data with multivariate statistics (i.e. Cluster Analysis, Principal Component Analyses and Linear Discriminant Analyses) were used to provide insights into the nature and provenance of the raw material. Potential geological raw materials for bricks manufacturing, were taken from modern floodplain (Nile alluvium) and calcareous clay deposits from lowland desert near the monument site, and subjected to chemical analyses, to compare them with the chemical composition of the studied bricks. Results show that the starting raw materials for bricks were probably obtained by mixing Nile alluvium (quarried from the Nile River floodplain deposits) with the possible introduction of a calcium carbonate-rich flux component as a temper. This will provide guidelines for future conservation strategy for making new compatible and durable bricks and/or materials to be utilized for restoration, and contributes to the preservation of the historical masonry under study.

Keywords: *Red Monastery, Historical bricks, Multivariate statistics, Provenance, Restoration.*

1. Introduction

Recently, architectural heritage preservation, as an interdisciplinary research area, attracts researchers' attention of many fields (e.g. archaeology, architecture, geology and Engineering). Geology and archaeology share the same aspects. They can achieve the different remnants of the past [1]. Burning bricks can be considered as a result of an artificial technique (natural or unnatural mixture of sediments which is transformed by low pressure process - high temperature). Thus, classical geological studies integr- ated with statistical analysis of geochemical data are powerful methods for describing the materials used in the red brick industry in order to infer the sources of potential raw materials and to model possible mixtures of components to maintain them. The Red Monastery (V-IV century AD) is one of the most important Coptic Orthodox monasteries in the Sohag Governorate, Egypt, which known as a sacred site since early christianity in Upper Egypt. The name of the monastery (red) is driven from the overall colour of

its construction material. The monastery itself has several churches. The Red Monastery lies about eight kilometers west of Sohag City at the extreme western edge of the cultivated land within a small village called El-Deir, fig. (1-a). The Red Monastery is surrounded by residential areas from the east and south and wastewater treatment plant and the newly reclaimed lands from west and north fig. (1-b). From an architectural point of view, the Red Monastery is very important for art architectural historians [2]. Over centuries, the Red Monastery historical building was threated by diverse damage and deterioration processes which are responsible for altering its building materials quality and characters. There are many factors which lead to such deterioration and degradation effects such as action of climate conditions, air pollution, groundwater rises, microorganisms, negligence (i.e. uses of inappropriate restoration materials by inadequate preservation techniques [3], rapidly increase of urbanization and agricultural expansion, the growth of pilgrims and visitors to the vulnerability places of the building and lack of financial supports for their restoration and conservation. Our study, describes the microstructure, geochemical, mineralogical composition and deterioration features of the Red Monastery wall bricks (to provide fundamental raw data on brick technology of such period of history). The main goals of this work are the determination of the possible provenance and probable raw materials used in the brick manufacturing as well as its possible firing technology. Also, we attempted to correlate the geochemical and petro-mineralogical composition to the deterioration features of the bricks to obtain valuable information for their future conservation and restoration plans by formulating a new brick/material using the proposed raw materials.
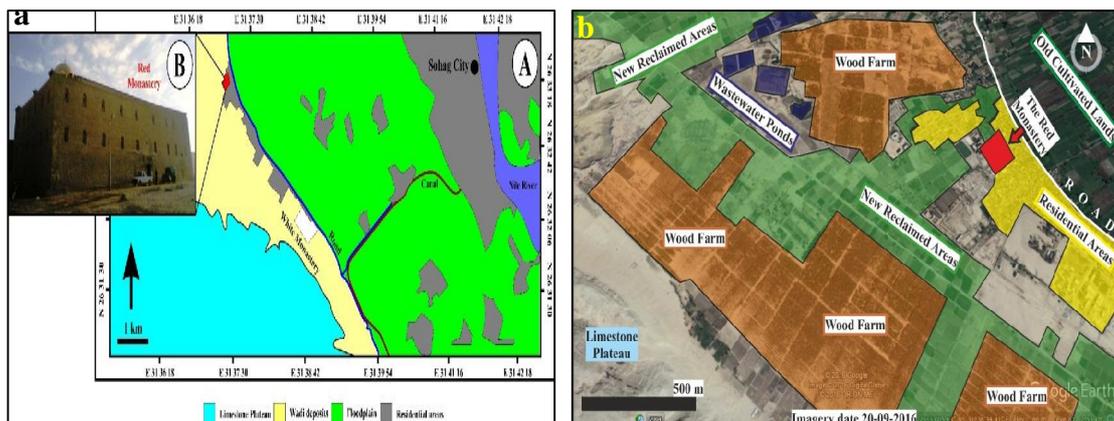

Figure (1) Shows **a**. a simplified map showing the Red Monastery location (A), and the monument under study (B) at Sohag, Egypt., **b**. Google image shows the different land uses occupied the study area nearby the Red Monastery

2. Geographic, Geological Setting and Climate

The Red Monastery, at El-Deir village, lies on the west bank of the Nile River about 400 km south of Cairo and about 10 km to the west of Sohag City (Lat 26°33'17.18"N, and long 31°37'11.29"E). The Red Monastery buildings located on the lowland desert area (altitude ranges between 70 and 140 m) bordered by the Eocene limestone plateau from the west and the cultivated modern floodplain land (altitude ranges between 55 and 65 m) from the east. The ground surface shows a general eastward slope toward the cultivated land, fig. (2-a). The Nile modern floodplain includes the nearby and levelled cultivated lands distributed along the eastern side of the site. Geologically, the various rock units distributed in Sohag area are entirely composed of sedimentary sequence ranging in age from Lower Eocene to Recent, fig. (2-b). There are Tertiary sedimentary rocks

(Eocene limestone, Pliocene clay) in the area. Subsequently, Pleistocene clastic sedimentary rocks and finally Quaternary sediments (modern floodplain and Wadi deposits) were formed. The main units are summarized in tab. (1). The study area is occupied by a thick succession of sandy and gravelly Pleistocene sediments covered with thin layer of the recent wadi deposits and it ranging in thickness from 1 m to more than 10 m [4], and broad areas of newly reclaimed lands which surround the site from the north and west. The area of study is characterized by a typical hot desert climate due to its geographic location. The wide variance of temperature, fig. (2-c) either monthly or yearly is affected greatly on the evaporation intensities. Sohag area is rainless region during summer and mild with rare rainfall in winter. The mean annual intensity of rainfall over the whole area reaches about 1.18 mm. Accordingly, the contribution of rainfall is very limited if compared with the losses by evaporation and evapo-transpiration. The evaporation rates are the function of air temperatures, relative humidity and wind speed. In general, the high rate of annual evaporation intensity (2395.2 mm/year [5] acts as a major factor of erosion and increases the relative humidity in the area. Worth mention, the evaporation intensity is more than the rainfall intensity, fig. (2-d,e). This reflects that the studied area suffers from aridity conditions. The relative humidity (RH) in Sohag ranges between 50 and 60 % in summer, where it reaches 33 to 35 % in winter [6]. The seasonally average of wind speed has somewhat higher rates in spring (3.6 – 5.6 km/hr), intermediate in winter and summer (3-6.3 km/hr) and low rates in autumn (2.3- 4.6 km/hr) during the period, 1977- 1992 [7]. The wind direction is variable during the year, while the predominant direction is north-west. From the view point of authors' examination, raw materials of the bricks are the modern floodplain and Wadi deposits which have the apparently proper in the physical properties (grain size distribution, clay content- plasticity) for brick manufacturing. The modern floodplain sediments are composed of Holocene fluviatile deposits consisting mainly of silt and clay. The recent wadi deposits include calcareous clay materials which are formed from the disintegrated products of the nearby Eocene carbonate limestone, mixed with reworked clayey materials from the preexisting sediments (derived from old river terraces and/or Pliocene clay). Hence, the wadi deposits are of local source and accumulated during successive stages of the local flash floods.

Table (1) main geological units in Sohag area [9]

| Age		Formation	Description	Ref
Neogene and Quaternary	Recent (Holocene)	Wadi deposits	Disintegrated product of the nearby Eocene carbonate, in addition to the reworked material from the pre-existing sediments	Said, 1975
		Alluvial deposits (Nile floodplain)	Clays and silts with sandstone intercalations	
	Pleistocene	Dandara	Fluviatile fine sand–silt intercalations and accumulated at low-energy environment	Omer and Issawi 1998
		Ghawanim	Nile sandy sediments exhibiting the first appearance of the heavy mineral	Omer 1996
		KomOmbo	Sand and gravel sediments containing abundant coarse fragments of igneous and metamorphic parentage	Butzer and Hansen 1968
		Qena	Quartozose sands and gravels lacking igneous and metamorphic fragments	Said 1981
	Late Pliocene / Early Pleistocene	Issawia	Clastic facies at the lake margins and carbonate facies in the central zones	Said 1975
	Early Pliocene	Muneiha	Bedded brown and gray clays intercalated with thin beds and lenses of silt and fine sand, and fluviatile-dominated sediments made up of sand, silt, and mud intercalations	Omer and Issawi 1998
Lower Eocene		Drunka	Medium to thick-bedded succession of limestone, which is highly bioturbated in some horizons, with siliceous concretions of variable sizes	Said 1960
		Thebes	Massive to laminated limestone with flint bands or nodules and marl rich with Nummulites and planktonic foraminifera	
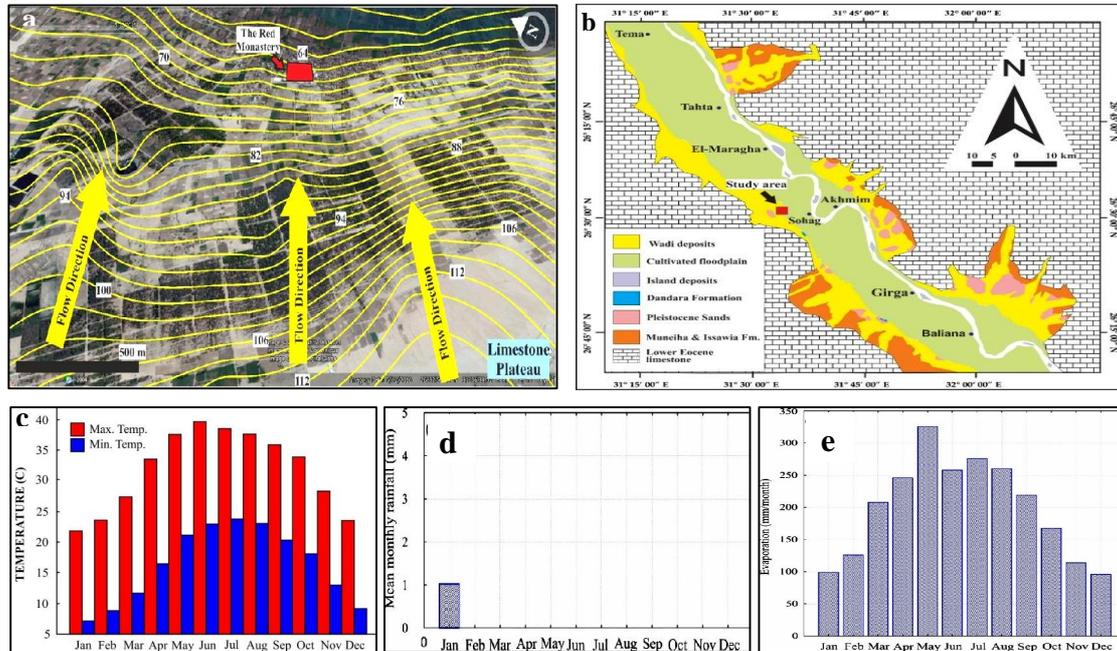
Figure (2) Shows **a**. ground surface contour map shows a general eastward slope and flow direction toward the study area and old cultivated lands, **b**. main geological units in Sohag area after [8], **c** column plot of mean daily maximum and minimum temperature, Sohag, Egypt [10], **d**. column plot of mean monthly amounts of precipitation [10], **e**. column plot of mean evaporation [11] - Sohag, Egypt.

3. MATERIALS AND METHODS

In this study, field observations are carried out during 2016 for Red Monastery to characterize the external

3.1. *Materials*

Several types of samples were collected from Red Monastery for investigate its current state. Five samples representative the brick units were randomly collected from the historical building during. In addition, 40 sediment samples were collected from local known sources around the Monastery to invest-

3.2. *Methods*

Bulk major element compositions of bricks and sediments were analyzed with XRF (using JEOL JSX-3222 ELEMENT ANALYZER, operating at 30 kV and 0.6 mA), Central Lab, South Valley Univ. The acidity was measured by means of a digital pH meter (Cole Parmer) in suspension (1 brick powder: 2.5 water) after 15 minutes of orbital shacking. Ten grams of brick sample (<63μ) were orbitally shaken with 50ml of distilled water for 15min. The extract was then filtered and used for measuring electrical conductivity (EC) and the soluble fraction of major cations

and deterioration features affected the bricks by standard and in situ visual inspections.

tigate the geological origin of the brick raw materials, a total of. Also, 30 Nile alluvium sediments from cultivated lands and 10 calcareous clay sediments from wadi deposits were used for source area comparison.

and anions (Ca^{2+}, Mg^2+, Na^+, K^+, HCO_3^-, Cl^-, SO_4^{-2} and NO_3^-). Mineral assemblages and textural characteristic of the bricks were studied on thin sections with an optical microscope, using an optical microscope coupled to a digital camera. The samples were cut and cold embedded in epoxy resin, and the resin blocks were sanded and polished in an automatic polisher. Mineral phases of low crystallinity could not be determined with the lower resolution of the petrographic microscope. To this end, the mineralogy of brick samples was prepared and measured by X- ray diffraction Philips PW 1820.

The raw data was processed using X'Pert High Score Plus version 2.1 software (PANalytical) to analyze the phases quantitatively by the relative intensity ratio method and identify the crystalline phases by comparison with diffraction patterns in the PDF2-ICDD database. The recording settings were: CuK =1.5405 A˚, 10 to 80° 2θ explored area, applying a step of 0.06º (2θ). This technique permits identification of the

3.3. Statistical treatments

The final major elements geochemical data, which consist of observations (*i.e. samples*) and variables (*i.e. elements*), have been treated using multivariate statistical methods. *Cluster analysis (CA)* is often used in the initial inspection of data because it is a rapid and efficient technique for evaluating relationships between a large numbers of samples, between which distance measures have been calculated [14]. CA classifies samples into distinct groups. The results are presented as *dendrograms* showing the order and levels of clustering as well as the distances/ similarity between individual samples. *Principal components analysis (PCA)* was then done to extract a minimum number of factors which explain satisfactory quantity of total variance of the data set. This analysis shows how variable the

mineral phases existing in the bricks and the presence or absence of diagnostic minerals. Micro textural relationships of the bricks were also examined with JEOL JSM- 5500 LV scanning electron microscope (SEM), Central Lab, South Valley Univ. The SEM offers evidence on firing temperatures based on the existence of glass phase that increases with the firing temperature and the duration of the firing [12,13].

samples are, and which variables drive the variance within the data set. Each variable included in the analysis is assigned an eigenvector score that reflects the positive or negative influence each has on the principal components as well as the strength of that influence. To further test the validity of the geochemical groupings and variability we performed a *canonical discriminant analysis (CDA)* on the statistical set for the major elements. In contrast to the PCA, the CDA test takes groups of samples with known differences and determines which variables (elements) contribute to those differences. The statistical analyses were performed with STATISTICA and MINITAB software packages.

4. RESULTS
5.1. Visual investigation

During the field observations of the historical building walls, different types of brick damages were evidenced. Figure. (3-a,b,c) shows the most common deterioration features of bricks, such as discolouration of many bricks, salt efflorescence; specially at wall foundations. Bird droppings and excrement, spalling, crumbling, weakness and collapse of bricks. Within the

same context, wearing out of mortar components at many places of walls could be noted. In addition to the presence of some minor deterioration symptoms. These symptoms such as powdering, reducing of sharp edges and corner roundness of bricks, rising damp and seepage of capillary groundwater and pitting.
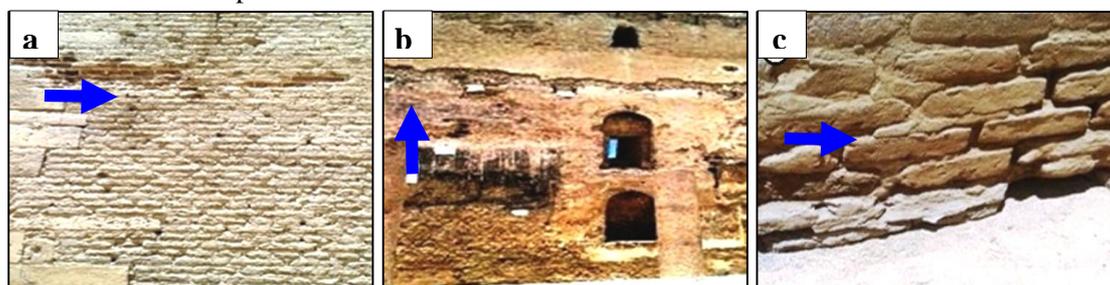

Figure (3-a,b,c) Shows different deterioration and degradation features affected the historical red bricks at the Red Monastery (*the arrow refer to the N*).

5.2. *Mineralogical analyses by optical microscope and XRD*

At the microscopic level, the Red Monastery bricks show number of mineral phases embedded in a cryptocrystalline to glassy ferruginous with low birefringence matrix. Among the mineral phases, newly formed Ca-rich plagioclase is the predominant feldspar phase, followed by epidotes and quartz, fig. (4-a,b, c,d,e,f). Quartz is observed in all thin sections, but much less abundant in the brick than in the precursor sediments i.e. Nile alluvium. Such observation can be explained by the fact that, the formation of new phases usually involves consumption of the primary phases as quartz, clay minerals and carbonates. In addition, the optical study revealed the presence minor amounts of prehnite and rare quantities of zoisite, apatite, tourmaline and opaque phases (iron minerals) as recorded by some authors [15,16]. Furthermore, the study indicates the absence of both clay minerals and calcite, although they are originally existing in the proposed raw materials. Absence of those phases was proved through XRD analysis, fig. (4-g). Referring to Ca-rich materials,

the decomposition of calcite to CaO and the reaction of the latter with free alumina and silica from breakdown of the clay determines the formation of high-temperature (850- 900°C) mineral phases i.e. diopside, gehlenite and anorthite [17,18]. The semi-quantitative mineralogical revealed no diffractions of lime (CaO) were found; yet, the patterns included those of gehlenite and diopside (of medium to weak inten-sity), those of hematite (very weak) and, particularly, those of anorthitic plagioclases (strong intensity). The former supposed process is supported by presence of bubbles (vugs) on the surface of the new anorthitic phase, fig. (4-e,f). In fact, there is a good association found between anorthite grains and large pores and vugs which originated from calcite decarbonatation during the-rmal cycle which leading to local calcium in high degree concentration and favors the in situ anorthite formation. In addition, presence of zoning in Ca-plagioclase indicates its formation under thermal effect.
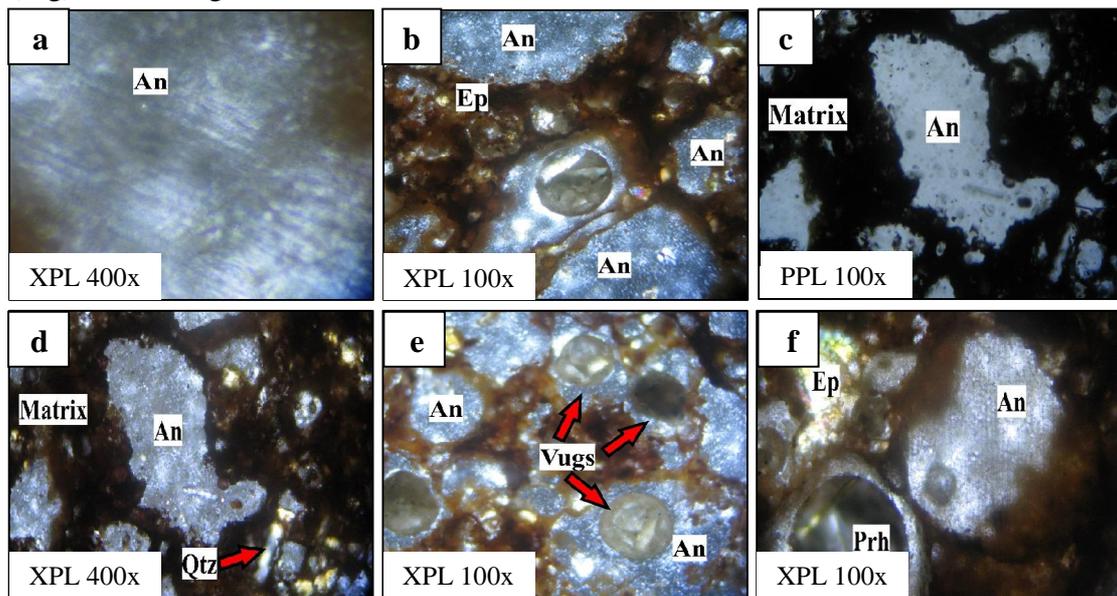

Figure (4) Shows photomicrographs of brick thin section between 100x and 400x in PPL and XPL **a**. porphyroblastic anorthite with distinct lamellar twins, **b**. coarse fabric containing large grains of anorthite stained with iron oxides. Note distribution of ca-Al silicate minerals through the matrix, **c**. & **d**. abundant, coarse porphyroblastic anorthite set in low birefringence ferruginous matrix and dark brown in color, **e**. microstructure is characterized by abundant vugs surrounded by newly formed anorthite aggregates, **f**. photo showing occurrence of epidote and prehnite as retrograde minerals preferently hosted in anorthite, dark brown and black amorphous phases are present; accessory minerals of apatite needle and fine tourmaline stand out in relief against anorthite surface under plane polarized light.
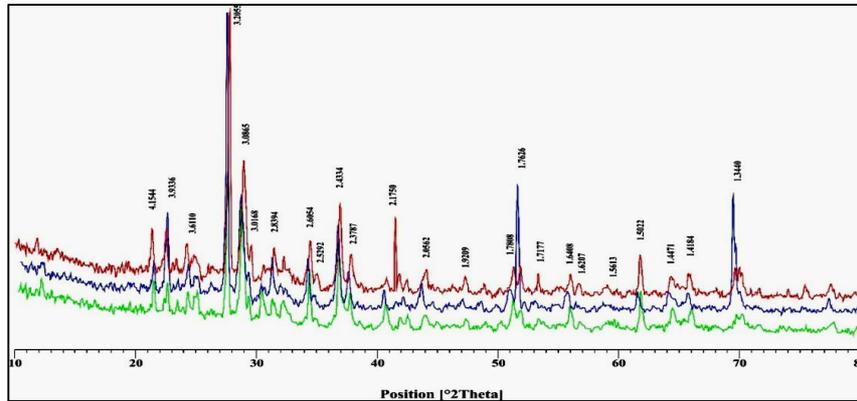
Figure (4-g) Shows XRD patterns of the studied brick samples from the Red Monastery historical building.

5.3. *Morphological features by SEM*

SEM photomicrographs indicate that the pore filling phases probably of Ca-Al silicates, fig. (5-a). Within the same context, the development of secondary porosity due to a partial verification of the matrix, fig. (5-b). The sample surfaces shown in fig. (5-c) become smoother and the pores become ellipsoid with smooth edges. Furthermore, the presence of tiny crystals possibly is mixture of calcium silicate (diopside) and calcium-aluminum silicate (gehlenite). In addition, another brick sample shows some mechanical deterioration features such as fissuring and micro-cracks.
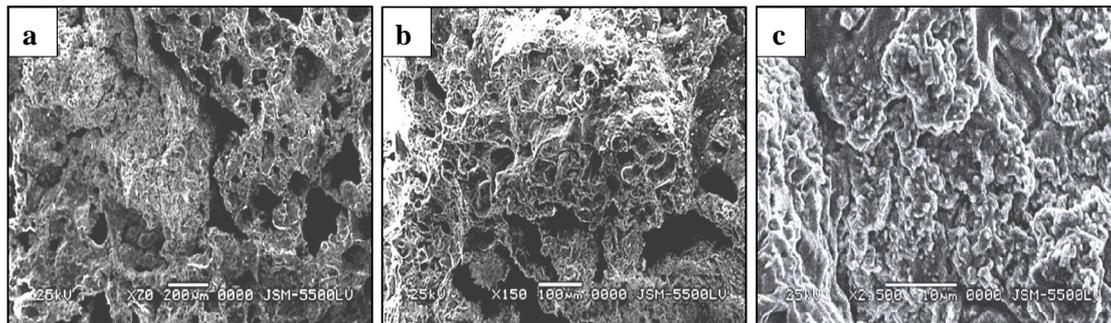

Figure (5) Shows SEM photomicrographs **a**. & **b**. partial vitrification of matrix displaying secondary porosity and vugs connected with rugous zones. Note the pore filling phases probably of Ca-Al silicates, **c**. tiny crystals of possibly a mixture of calcium silicate (diopside) and calcium-aluminum silicate (gehlenite), brick shows fissuring and micro-cracks on the lift side. the development of secondary porosity due to a partial verification of the matrix.

5.4. *Bulk chemical composition and geochemical provenance of fired brick*

The bulk chemical composition of the fired bricks (n=5) contains 45.67 to 62.57 % of silica with an average of 54.20 % whereas alumina ranges from 8.49 to 16.23 % with an average of 13.24 %. The average variability of SiO_2 and Al_2O_3 exhibit low standard deviation indicating the relatively homogeneous of the chemical components base of raw material used on brick manufacture. The studied of the red bricks show a significant content of CaO ranges from 8.16 to 18.49 % with an average of 11.79 % most likely due to artificially Ca-rich materials addition. The high Ca content maybe explained by the original Ca-rich raw materials or artificially addition of Ca-rich materials. In fact, this high Ca concentration in the bricks relative to the Nile sediments (average 4.80 %) clearly indicates that the baking paste of the red bricks is different from those of the Nile alluvium. Furthermore, the differences are too great to assume that the bricks were made only from Nile sediments. The calcareous clay deposits from the wadi deposits are characterized by a high percentage of Ca-salts (i.e., $CaSO_4$

and $CaCO_3$) and these may have been mixed with some Nile alluvium to form the baking paste of our bricks. The SiO_2, Al_2O_3 and K_2O content of the studied bricks is generally lower than that of the local Nile alluvium, maybe due to dilution by added temper materials to Nile alluvium. The presence of low K_2O content indicates the presence of small amount of illite in materials of original raw. Combined with the XRD results, fig. (4-g) and the chemical analysis, tab (2) & fig. (6-a), it could be confirmed that samples contain quartz ($SiO_2>$ %-50 %) indicates that this mineral has already found in the original raw material. This high Ca/Al ratio in the studied brick samples (0.89) relative to that of the Nile sediments (0.33) suggests that Ca rich salts (i.e. $CaCO_3$) were mixed with the Nile sediments to form the baking paste of the bricks. The addition of

Ca salts to the clay raw materials would lead to rapid extensive vitrification in the 800 to 850°C temperature range. Based on the XRD results and the principal oxides content, the rough mineralogical composition of the bricks can be refigured, as shown in the CaO+ (FeO+ MgO)-Al_2O_3-SiO_2 ternary phase diagram illustrated, fig. (6-b). The new formation mineral phases (i.e. anorthite, diopside and gehlenite) agree with the phase equilibrium diagrams, though they do not reach their equilibrium conditions. Thus, gehlenite (CaO· Al_2O_3·SiO_2) reacts with quartz to form diopside (CaO.MgO. $2SiO_2$) and anorthite (CaO.Al_2O_3.$2SiO_2$). Most of the studied brick compositions fall in the quartz-diopside-anorthite triangle, whereas only one sample with higher CaO falls in CaO·SiO_2, CaO.Al_2O_3.$2SiO_2$, 2CaO.Al_2O_3.SiO_2 (diopside, anorthite, gehlenite) compatibility triangle.

Table (2) summary statistics of XRF results for the major oxides composition of the studied three geochemical groups.

Variable	Values %.						
	Group	*Mean*	*StDev*	*Variance*	*Minimum*	*Medium*	*Maximum*
SiO_2	CC	51.69	7.55	57.05	38.90	52.59	63.45
	NS	60.45	5.62	31.60	42.80	60.28	72.41
	RB	54.20	6.69	44.70	45.67	56.30	62.57
Al_2O_3	CC	16.18	3.94	15.55	12.42	14.70	23.50
	NS	14.76	1.75	3.05	10.69	14.90	20.16
	RB	13.24	3.01	9.05	8.49	14.04	16.23
CaO	CC	16.13	3.24	10.48	10.00	16.53	20.10
	NS	4.80	2.61	6.81	2.71	3.96	16.20
	RB	11.79	4.15	17.25	8.16	11.22	18.49
MgO	CC	2.78	0.67	0.45	1.76	2.93	3.48
	NS	2.76	0.40	0.16	2.05	2.70	3.58
	RB	9.16	2.15	4.60	6.80	10.16	11.33
Na_2O	CC	1.15	0.38	0.14	0.39	1.29	1.52
	NS	1.58	0.27	0.07	0.92	1.52	2.21
	RB	1.78	0.38	0.14	1.47	1.57	2.21
K_2O	CC	1.59	0.36	0.13	1.09	1.75	2.06
	NS	2.02	0.69	0.47	1.27	1.84	4.05
	RB	1.48	0.40	0.16	1.08	1.35	2.14
FeO_3	CC	7.29	1.13	1.28	5.45	7.14	9.09
	NS	9.58	1.08	1.17	7.14	9.76	11.91
	RB	10.43	2.41	5.82	7.75	11.49	13.12
MnO	CC	0.12	0.05	0.00	0.04	0.13	0.20
	NS	0.15	0.03	0.00	0.10	0.16	0.19

	RB	0.65	0.19	0.04	0.45	0.60	0.88
	CC	1.07	0.27	0.07	0.68	1.05	1.49
TiO$_2$	NS	1.71	0.26	0.07	1.06	1.72	2.24
	RB	2.52	0.72	0.52	1.58	2.45	3.39
	CC	0.66	0.40	0.16	0.16	0.55	1.48
P$_2$O$_5$	NS	0.57	0.27	0.07	0.23	0.53	1.23
	RB	2.15	0.73	0.53	1.07	2.51	2.86

CC=calcareous clay sediments (n=10); NA=Nile alluvium sediments (n=30); RB=Red Brick samples (n=5).
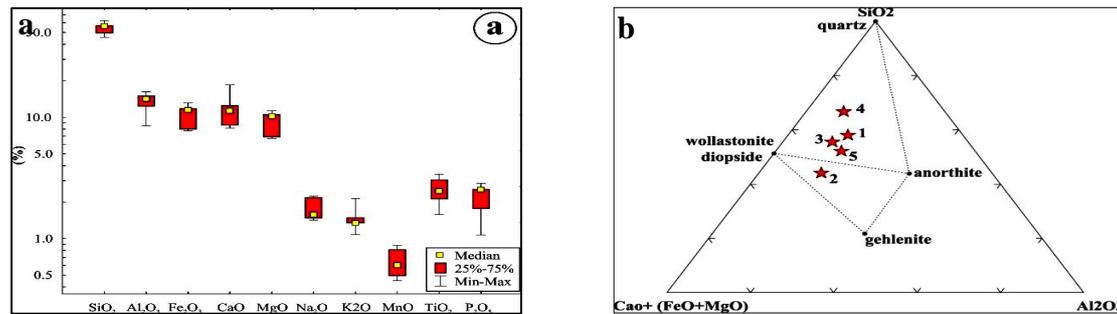

Figure (6) Shows **a**. box–whiskers graph of different geochemical data explaining the lower, median and upper quartile, maximum and minimum values of 10 bulk major and minor oxides (%), **b**. and content of soluble cations and anions in ppm, **c**. schematic representation of the composition of the brick samples in the CaO+(FeO+MgO)-Al$_2$O$_3$-SiO$_2$ phase diagram

5.5. *Water extracted soluble salts and their sources*

Based on chemical analysis of extracts from brick samples, tab. (3) & fig. (7), the order of abundance of the major cations is Na$^+$ > Ca^{2+} > K$^+$ > Mg^{2+}, while that of anions is Cl$^-$ > SO4^{2-} > HCO3$^-$ > NO3^{-}. XRD and XRF results indicated halite (NaCl), Nitratine (NaNO$_3$), Kalicinite (KCO$_3$) and two sulphates gypsum (CaSO$_4$.2H$_2$O) and polyhalite (K$_2$Ca$_2$Mg (SO$_4$)$_4$(H$_2$O)$_2$) minerals. It can be deduced that in addition to mineral phases identified by XRD technique other soluble solid phases must be present as expected from the hypothetical salt combination modelling; e.g. Sylvite (KCl), magnesium sulphate (MgSO$_4$) and nitre (KNO$_3$).

Table (3) contents of soluble cations and anions in the analyzed brick sample.

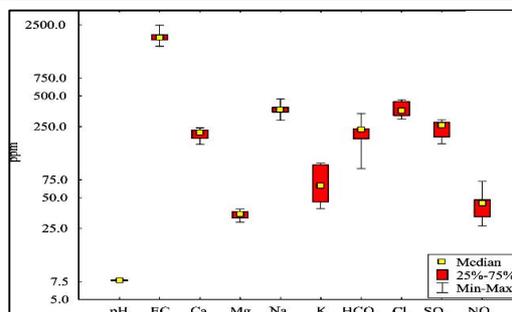| Chemical Characteristics			Samples				
			1	*2*	*3*	*4*	*5*
Soluble salts	Cations	Ca	245	219	192	169	234
		Mg	39	32	35	37	29
		Na	467	346	287	387	368
		K	106	65	105	45	39
	Anions	Cl	443	297	320	452	356
		SO$_4$	277	255	170	198	293
		HCO$_3$	336	97	190	234	239
		NO$_3$	73	44	27	32	48
pH			7.78	7.61	7.83	7.59	7.90
TDS			1986	1355	1326	1555	1606

Figure (7) Shows content of soluble cations and anions in ppm

5. Discussion

Numerous threats were supposed to impact the Red Monastery. These threats include agricultural expansion; municipal wastewater treatment ponds and the attached woody areas; increasing urban areas surrounding the monastery; climatic deterioration; and man-made impacts by inadequate restoration. These factors may damage and impact the wall bricks. Examination of space images, fig. (2-a) revealed an increase in reclamation activities in the area. This expansion resulted in increasing irrigation which done without suitable drainage network. The northern and western directions from the Monastery are occupied by wastewater ponds and lagoons as well as the attached tree farms. Uncontrolled residential sprawl surrounds the Monastery from both eastern and southern directions also catastrophically threat its buildings. The leakage from irrigation water, domestic wastewater and evaporation ponds is the major source of groundwater recharge in the study area raising its level. The domestic wastewater characterized by high total soluble salts content especially chlorides and N-compounds which reacts with the lower parts of the building walls causing several damages and deterioration of bricks such as peeling, weakness and collapse of bricks, fig. (3-a,b,c). In addition, the principal air threats associated with wastewater treatments are emission of hydrogen sulfide and chlorine gases through biochemical reactions in ponds and leakage from tanks respectively. These gases form acids especially in the presence of moisture. In the initial stage, which is represented by the core of the crystal, there was relict material of the original components and the formed crystals are still weak. In the latter stages the growing crystals become gradually stronger and gain more of their characteristics (e.g. crystal form and size). SEM examination shows recrystallization of minute crystals from the vitreous phases probably a mixture of Ca silicates (e.g., diopside) and/or Ca-Al silicates (e.g., gehlenite), fig. (5), the situation makes them difficult to identify under polarizing microscope but easy to characterize by XRD. High temperature mineral phases e.g. mullite or cristobalite were neither detected in SEM micrographs nor XRD patterns. The matrix is dark brown in color with abundant brownish-red amorphous phases and sometimes display grains of epidote, fig. (4). The common vitreous phases are isotropic under crossed nicols and proved by the rising of the background noise in the XRD data and SEM investigations. The studied sections also are characterized by abundant oval to rounded vugs resulted from degassing of the CO_2 from carbonate decomposition [19]. Such vugs are totally or partially filled with tiny crystals of new formed colourless prehnite characterized by its low relief and distinctive bow tie crystal form. Integration of mineralogical findings (i.e. petrographic, XRD and SEM analyses) with minerals transformation and their thermal stabilityies data obtained from literatures e.g. [20,21,22]; can be used for esteeming the firing temperature as well as the behavior of the raw material used in the bricks manufacturing [23] considering its mineralogical composition. For example, montmorillonite and kaolinite clay minerals are originally present in the Nile alluvium sediments [4] and are not present in any of the studied brick samples, clearly indicates the firing temperatures for the brick samples studied exceeded 700°C result in their decomposition with release of free silica and alumina. In the interval of 600 to 800°C, carbonates completely decomposed [24], giving rise to the formation of free lime (CaO). At approximately 700°C, metastable gehlenite (2CaO. $Al_2O_3.SiO_2$) starts to form due to the reaction of free alumina and silica with lime [25]. Gehlenite is not a common mineral in the Nile deposits and is stable in the 800 to 900°C tempe-rature range in which its presence indicates that the firing temperature did not exceed 900°C [26]. Vitrification starts at relatively lower temperature (~ 800°C)

when car-bonates are present [27]. The considera-ble content of CaO (11.79 %) and MgO (9.16 %) from added carbonates act as fluxing agents [28] caused the amorphous phases founded, fig. (5). The metastable calcium silicates (diopside) appear in the range 850–900°C [17,29]. At this temperature, anorthite starts to form at the expenses of free alumina and silica (plus quartz) as reported by Cultrone [22]. The predominance of anorthite indicates that its formation temperature residence time was relatively longer. In addition, the absence of phases like mullite and/or cristobalite peaks indicates that the bricks had been burnt at low firing temperature and did not exceed 900°C [30]. During cooling of bricks induces fracturing allowing the influx of H_2O/CO_2 rich fluids under relatively high pressure resulting in formation of retrograde assemblages of hydrous Ca-Al silicates minerals e.g. epidote and prehnite. The consuming reactions of anorthite released Ca and Al which are responsible for former minerals formation which formed in pore spaces and vesicles, or within the anorthite itself. Dependent upon results of this study and on the literature, it can be concluded that favoring temperature of raw material baking pastes used in manufacturing of the bricks did not exceed 900°C. Overall, it seems that the craftsmen's experience of brick technology and manufacturing allowed them to produce bricks by adding or mixing Ca rich sediments to the Nile alluvium deposits. This new bricks seems to have been quite pleasant, since craftsmen preferred to produce it rather than bricks formed from Nile alluvium or calcareous clay materials alone. Such technique was known by the Romans, who prefer Ca-rich sediments for their ceramics (both fine and coarse) than the more abundant lime-free deposits [29]. To discriminate calcareous clays from Nile alluvium, it is not appropriate to employ trace element analysis [31]. The statistical treatment of the studied bricks based on major oxides geochemical data resulted

in formation of two distinct groups for Nile alluvium and calcareous clays deposits, with the bricks showing a relatively distinct group between their chemical characteristics as discussed below. *Cluster analysis* was first applied to the geochemical dataset. The resulting dendrogram is noticed in fig. (8-a). using single linkage as a grouping rule according to Euclidean distances and there are three clusters. Cluster (1) contains 30 samples (Nile alluvium sediments), cluster (2) contains 5 samples (red bricks) and the third contains 10 samples (calcareous clay sediments). The methodology successfully recognized the brick samples as a unique group when compared with entire data set. Figure (8-b) shows that there are three factors extracted by PCA explain 77.9 % of the total variance of the data set. Loadings of the 1st and 2nd factors successfully differentiated the study chemical parameters (*R-mode PCA*) into three distinctive geochemical trends, fig. (8-c) reflecting their possible related sources: Ca-poor sediments (i.e. Nile alluvium), Ca-rich sediments (i.e. calcareous clay) and Mixed trends (our brick samples). Table (4) displays the factor loading for the three extracted factors. The first PC explains 40.03 % of the total variance in the data set. The elements that positively drive the variance are Ti, Mn, Fe, P, Mg and Na, likely because they are associated directly with floodplain sediments and temper composition. The Ca negatively drive the variance within the sample set which are the principally associated with the artificial addition of carbonate materials to the parent rock and hence play as a diluter. PC2 explains the high positive loadings of elements Ca, Mg and Mn with the total variance of 22.04 % forming a pronounced Ca-rich sediment trend. Finally, PC3 explains the total variance is about 15.84 % and the high positive element is Al followed by Na, K, Fe, Mn and Ca. This association is lithologically controlled and corresponds to Ca-poor sediments. The studied floodplain sediments composed of clay minerals (Al+

K), feldspars (Ca+Na) and ferromagnesian minerals (Fe). In addition, the inter-sample relationship was statistically evaluated using the *Q-mode* technique, fig. (8-d). This technique produced results similar to CA, fig. (8-a) that showing three different geochemical groups illustrating the ele-ments which drive the variance within the set. Figure (8-e) summarizes the CDA results show majority of the samples fall within the same clusters of geochemical group which identified by PCA and CA. The CDA plots the unknown brick samples and each of locale sedim-ent types separately and uniquely into distinct groups. The brick samples of unknown provenance do not assign directly to any sediment type but are most closely related to that Nile alluvium sediments group. This may be due to addition of Ca-rich sediments from local sources into the Nile alluvium sediments as a flux

and/or temper materials, resulting in a very small range of geochemical signat-ures. The origin of water soluble salts in bricks is mostly extrinsic, which transp-orted into the bricks from their surrounding environment. Sodium chloride usually penetrates brick from the soil through damp rising. Nitrate salts are often attributed to cultivated lands and agric-ultural practices around the study area which release N-compounds to ground-water capillary rise. Sulphate ions are observed in air polluted environments and/or ascribed to surrounding mortar. The occurrence of these soluble ions indicates that the bricks suffer from many enviro-nmental factors leading to their deterior-ation and damage. Soluble salts crystallize to many mineral phases generating micro-cracks in the bricks, fig. (5) lowering their physical and chemical properties.
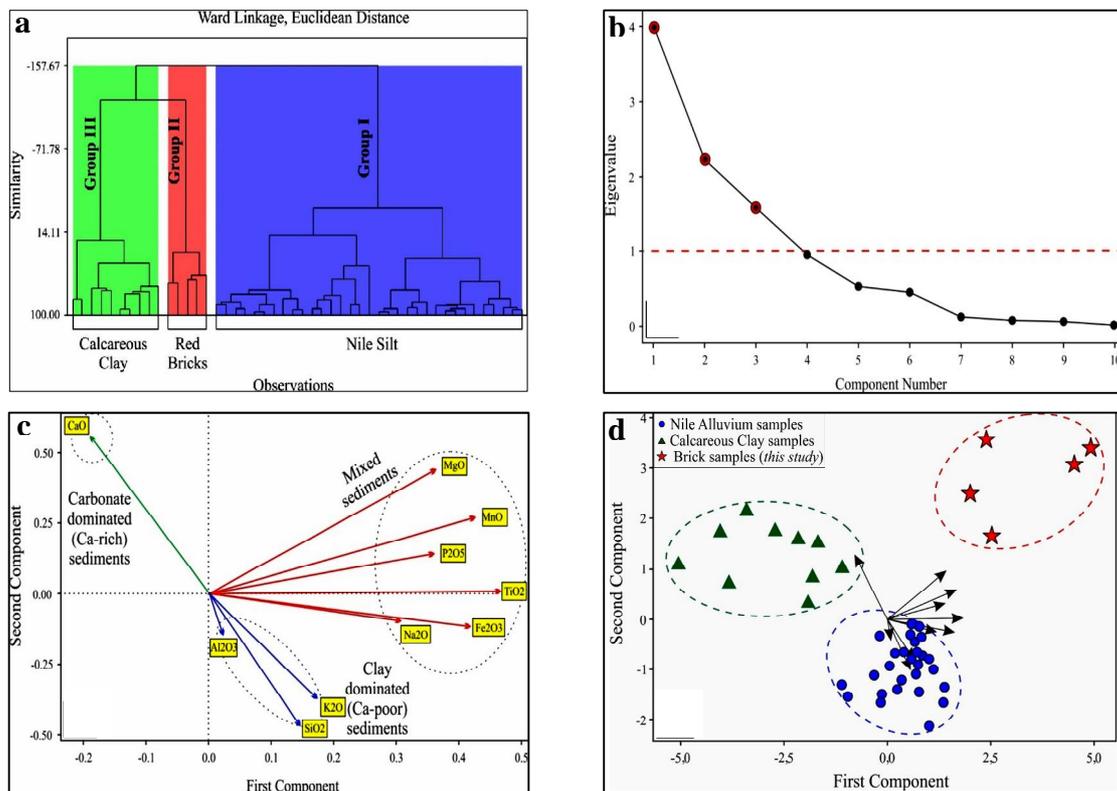

Figure (7) Shows **a**. Cluster analysis dendrograms (ward linkage, squared Euclidean distance) of XRF geochemical results for the studied samples, **b**. values of the different eigenvalues Illustrating the first three components which are the most effective ones, the red circles explains the three retained components and the horizontal line shows an eigenvalue of 1, **c**. R-mode component loadings calculated for measured variables for the studied sediments and bricks from the study area, **d**. Q-mode PCA graph illustrating relationship between the two sediment types (Nile alluvium and calcareous clay) and the mixed source-brick samples composed of material derived from these two sediments.

Table (4) loadings of the PCA eigenvectors for the first three components

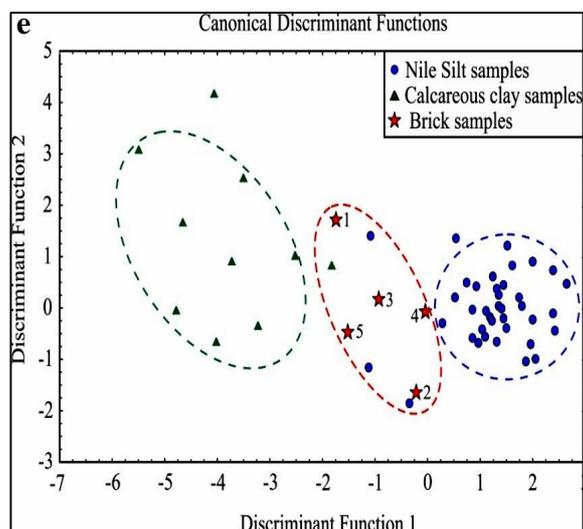| Variable	PC1 Mixed	PC2 Carbonate	PC3 Clay
SiO_2	0,143	-0,460	-0,504
Al_2O_3	0,021	-0,136	0,683
CaO	-0,196	0,578	0,135
MgO	0,359	0,435	-0,085
Na_2O	0,303	-0,096	0,333
K_2O	0,169	-0,367	0,141
Fe_2O_3	0,414	-0,117	0,275
MnO	0,422	0,264	-0,203
TiO_2	0,463	0,008	-0,024
P_2O_5	0,357	0,141	-0,076

Figure (8-e) Shows canonical discriminant plot explain the three different geochemical groups.

6. Treatment Recommendations

The damage products that are related to or are often attached to the different types of surfaces are varied according to the damage caused to them. Based on the multiple damage, there are many methods, methods and materials used to remove the various forms of damage. Prior to the start of cleaning methods, the objective or purpose of cleaning is first identified. There are many important and important reasons for cleaning parts. Detecting and highlighting the aesthetic values of the red monastery, cleaning is a necessary work in the restoration. Cleaning here means the removal of harmful components from surfaces such as water-soluble salts and many pollutants. Cleaning is also an important step to prepare the surface for consolidation. Soil, mud calcification, and salt layers deposited on the surface can be removed using soft and coarse brushes, cutters and furs, metal, and wood. Also, modern methods using dry granular extrusion or dental drill machines were also utilized. It was believed that poultices were the most appropriate method of removing salts and mud calcification. Chemical cleaning was also used to remove iron rust stains using a 2 % solution of hydrofluoric acid. Additionally, the soil could be cleaned with a small amount of alkaline soap, (100 g soap, 100 cm 3 water, and 10 cm 3), but soap and ammonia should be removed. The foundations must be isolated from the soil to prevent access to ground water. Sewerage system must also maintain water network around the monastery. It was also necessary to create a network, aiming to reduce the level of ground water constantly, especially as the monastery is located at a low level of the surrounding reclaimed land and the surrounding tree farm, making it vulnerable to many different manifestations of damage. It was necessary to consolidate the brick structure damaged according to the rate of damage that could be used with the red brick of the monastery of calcium hydroxide, barium hydroxide or suitable polymer.

7. Conclusion

The study of the bricks from the historical site of Red Monastery (Sohag, Egypt) suggests that the raw clayey material used in the making of the bricks were of local origin, and came from sediments nearby the Monastery. Integration of the XRF results with the proper statistical analysis was successful in identifying two mixed geochemical signatures of the studied bricks,

non-calcareous and calcareous sediments. It seems that these early craftsmen quarried the raw materials in two main areas, one of which was poor from the eastern cultivated lands (i.e. Nile alluvium) and the other was rich in carbonates from the wadi deposits (i.e. calcareous clay) located west of the Monastery. On the basis of the mineralogical analysis and literatures we estimated the firing temperature was around 900°C. Our findings are important to clarify technological achievements and raw material sources of early civilizations which can be used to select appropriate raw composition and firing temperatures for new bricks used in conservation-restoration interventions of the Monastery under study and other historical buildings of the same period and location. The brickwork in the Red Monastery requires physical protection against decay and natural erosion. Tile above the monastery should be tilted enough that represents adequate protection from rain. Therefore, weather proof material, e.g. fluoro - polyethers polymers with large partial installation should be utilized. It dissolves into Trichloro - Trifluoro - Ethan to achieve a balance between the absorption, distribution, and evaporation of bricks.

References

[1] Szilágyi, V., Gyarmati, M., Tóth, J., Taubald, H., Balla, M., Kasztovszky Zs. & Szakmány, Gy., (2012). Petro-mineralogy and geochemistry as tools of provenance analysis on archaeological pottery: Study of Inka period ceramics from Paria, Bolivia. *Journal of South American Earth Sciences*, Vol. 36, pp: 1-17.

[2] Bolman, E., (2009). Reflections on the Red Monastery project: 2000-2008, *Bulletin of the American Research Center in Egypt,* Vol. 194, pp: 9-13.

[3] El-Gohary, M., (2007). Degradation of limestone buildings in Jordan: Working effects and conservation problems: "A critical study according to international codes of practice", *Adumatu*, Vol. 16, pp. pp: 7-24.

[4] Omer, A., (1996). *Geological, mineralogical and geochemical studies on the Neogene and Quaternary Nile basin deposits, Qena-Assiut stretch, Egypt,* Ph.D., Geology dept., Faculty of Sciences, Sohag, South Valley Univ., Egypt.

[5] Abdel Rahman, A., (2006). *Hydrogeological and geophysical assessment of the reclaimed areas in Sohag, Nile Valley, Egypt*, Ph.D., Geology dept., Faculty of Sciences, Ain Shams Univ.

[6] Egyptian Meteorological Authority, (2000). *Meteorological data base.* Yearly report, Cairo, Egypt.

[7] Ahmed, A., (1997). *Geophysical and hydrogeological studies in the area southeast of Sohag, Egypt*, M.Sc., Geology dept., Faculty of Sciences. Sohag, South Valley Univ., Egypt.

[8] Ali, M., (2005). *Geochemical characteristics of the surficial Nile basin sediments and their environmental relevance, Sohag area, Egypt*. M.Sc., Geology dept., Faculty of Sciences, South Valley Univ., Egypt.

[9] Youssef, A., Omer, A., Ibrahim, M., Ali, M. & Cawlfield, J., (2011). Geotechnical investigation of sewage wastewater disposal sites and use of GIS land use maps to assess environmental hazards: Sohag, upper Egypt, *Arab J. GeoSci*, Vol. 4, pp: 719-733

[10] Allmetsat (2008). http://en.allmetsat.com/climate/egypt.php?code=62397, Climate: Sohag, Egypt. (12/6/2016)

[11] Gomaa, M., (2003). Groundwater quality of the Quaternary aquifer in Assiut area, Egypt, *Jour. Environ. Sc., Mansoura Univ.*, Vol. 26 (1), pp: 163-185.

[12] Tite, M., Maniatis, Y., (1975). Examination of ancient pottery using the scanning electron microscope, *Nature*, Vol. 257 p122-123

[13] Tite, M., Freestone, I., Meeks, N. & Bimson, M., (1982). The use of scanning electron microscopy in the technological examination of ancient ceramics, in: Olin, J. & Franklin, A. (eds.) *Archaeological Ceramics*, Smithsonian Institution Press., Washington, DC., pp: 109-120.

[14] Bieber JR, A., Brooks, D., Harbottle, G. & Sayre, E., (1976). Applicatin of multivariate techniques to analytical data on Aegean ceramics, *Archaeometry*, Vol. 18 (1), pp: 59-74

[15] Ghergari, L., Ionescu, C. & Horga, M., (2003). Mineralogy of ceramic artifacts from Ilisua archaeological site (Bistrita-Nasaud County, Romania).

Studii si Cercetari Geologie,Geografie, Vol. 8, pp: 129-137.

[16] Horga, M., (2008). *Geoarchaeological studies on ceramics and lithics from archaeological sites from (Bistrita-Nasaud County, Romania).* Ph.D., Babes-Bolyai Univ. of Cluj-Napoca, Romania

[17] Maggetti, M., (1982). Phase analysis and its significance for technology and origin, Olin, J. & Franklin, A. (eds.) *Archaeological Ceramics*, Smithsonian Institution Press., Washington, DC., pp: 121-134.

[18] Maggetti, M., Westly, H. & Olin, J., (1984). Provenance and technical studies of Mexican majolica using elemental and phase analysis, in: Lambert, J., (ed.) *Archaeological Chemistry*-III, American Chemical Society, Washington, D.C., pp: 151-191

[19] Robinson, G., (1982). Characterization of bricks and their resistance to deterioration mechanisms, in: *Conservation of Historic Stone Buildings and Monuments*, National Academy Press, pp. 145-162.

[20] Jordán, M., Martín-Martín, J., Sanfeliu, T., Gómez-Gras, D. & de la Fuente, C., (2009). Mineralogy and firing transformations of Permo-Triassic clays used in the manufacturing of ceramic tile bodies, *Applied Clay Science*, Vol. 44 (1-2), pp: 173-177.

[21] Trindade, M., Dias, M., Coroado, J. & Rocha, F., (2009). Mineralogical transformations of calcareous rich clays with fi ring: A comparative study between calcite and dolomite rich clays from Algarve, Portugal, *Applied Clay Science*, Vol. 42: pp: 345-355.

[22] Cultrone, G., Rodriguez-Navarro, C., Sebastián, E., Cazalla, O., De La Torre, M., (2001). Carbonate and silicate phase reactions during ceramic firing, *Eur. J. Mineralogy*, Vol. 13 (3), pp: 621-634.

[23] Barbera, G., Barone, G., Crupi, V., Longo, F., Maisano, G. & Majolino D., (2013). Small angle neutron scattering study of ancient pottery from Syracuse (Sicily, Southern Italy), *J. Archaeol Sci.*, Vol. 40 (2) pp: 983-91.

[24] Mercury, J., Costa Pereira, D., Vasconcelos, N., Cabral Jr, A. & Angélica, R. (2013). Chemical and mineralogical characterization of Portuguese ceramic tiles in the historic center of São Luís do Maranhão (Brazil): An approximation of the mineralogy and firing temperature of the raw materials, *Metalurgia e materiais*, Vol. 66 (1), pp: 91-98.

[25] Capel, J., Huertas, F. & Linares, J., (1985). High temperature reactions and use of Bronze Age pottery from La Mancha. Central Spain, *Miner. Petrogr. Acta*, Vol. 29-A, pp: 563-575.

[26] Riccardi, M., Messiga, B. & Duminuco, P., (1999). An approach to the dynamics of clay firing, *Appl. Clay Sci.*, Vol. 15 (3-4), pp: 393-409.

[27] Tite, M. & Maniatis, Y., (1975). A scanning electron microscope examination of the bloating of fired cáliz, *Transactions of the British Ceramic Society*, Vol. 74, pp: 229-232.

[28] Segnit, E. & Anderson, C., (1972). Scanning electron microscopy of fired illite, *Transactions of the British Ceramic Society,* Vol. 71, pp: 85-88.

[29] Peters, T. & Iberg, R., (1978). Mineralogical changes during firing of calcium-rich brick clays, *Am. Ceram. Soc. Bull.*, Vol. 57, pp: 503-509.

[30] Cardiano, P., Ioppolo, S., De Stefano, C., Pettignano, A., Sergi, S. & Piraino P., (2004). Study and characterization of the ancient bricks of monastery of "San Filippo di Fragalà" in Frazzanò (Sicily). *Analytica Chimica Acta*, Vol. 519 (1), pp: 103-111.

[31] Hancock, R., Millett, N. & Mills, A., (1986). A rapid INAA method to characterize Egyptian ceramics, *J. of Archaeological Science*, Vol. 13, pp: 107-117.